

# Electronic Structure of $\text{SrBi}_2\text{Ta}_2\text{O}_9$ Powders

Akihiko Shimizu, Syozo Takada, Hirokazu Shimooka, Seiji Takahashi, and Shigemi Kohiki\*

Department of Materials Science, Kyusyu Institute of Technology, Tobata,  
Kita-kyusyu 804-8550, Japan

Masao Arai

National Institute of Materials Science, Tsukuba, Ibaraki 305-0044, Japan

Masaoki Oku

Institute for Materials Research, Tohoku University, Sendai 980-8577, Japan

Received May 7, 2002. Revised Manuscript Received July 4, 2002

X-ray diffraction, Raman scattering, and X-ray photoemission of  $\text{SrBi}_2\text{Ta}_2\text{O}_9$  powder sample (the Curie temperature of 310 °C) synthesized from a precursor solution showed that the crystal structure of the  $\text{SrBi}_2\text{Ta}_2\text{O}_9$  unit cell was preserved from bulk to surface, and the surface had never been covered with metallic Bi and/or  $\text{Bi}_2\text{O}_3$ . The theoretical valence band spectrum, derived from the density of states by full-potential linearized augmented plane-wave computation and the photoionization cross section, reproduced well the experimental valence band spectrum. The computation revealed that the valence band maximum is dominated by the O p states and that the low-energy part of the conduction band is formed from the Bi p and Ta d states hybridizing with the O p states. In the vicinity of the conduction band minimum, the hybridization between Bi p states and Ta d states is weak and the Bi p states have slightly lower energy than the Ta d states.

## I. Introduction

Despite great efforts in thin film technology to fabricate ferroelectric random access memory devices,<sup>1</sup> a few attempts have been made to clarify in detail the electronic structure of  $\text{SrBi}_2\text{Ta}_2\text{O}_9$  (SBT). Robertson et al.<sup>2</sup> calculated the band structure of SBT by the tight-binding (TB) method with the parameters based on  $\text{PbTiO}_3$ . They used an orthogonal basis of O p, Ta d, and Bi s and p orbitals, though no orbital for Sr was considered. The calculated valence band (VB) width was ≈6.5 eV. Using X-ray photoemission spectroscopy (XPS), they measured the experimental VB spectrum with the estimated width of ≈7.5 eV for a SBT thin film fabricated by the process of metal–organic decomposition (MOD) and ozone treatment at 400 °C and concluded that the calculated density of states (DOS) by the TB method reproduced well the electronic structure of SBT. Hartmann et al.<sup>3</sup> reported the experimental VB width of ≈7.5 eV for a SBT film which was spin-coated on a Pt electrode and heated at 800 °C in oxygen. Watanabe et al.<sup>4</sup> reported the experimental VB with an estimated

width of 7 eV by XPS for the SBT films with nonstoichiometric compositions in both bulk and surface. The films were spin-coated on Pt electrodes and heated at 800 °C in oxygen. For the VB spectra the films with different compositions showed no apparent differences ascribable to the Bi s and p states in the TB-calculated DOS. However, the intensity of the Bi 6s semicore state was obviously enlarged for the Bi-rich SBT film with  $\text{Sr:Bi:Ta} = 1.0:3.2:2.0$ . Recently, Stachiotti et al.<sup>5,6</sup> reported the electronic structure of SBT from first principles within the local-density approximation (LDA) using the full-potential linearized augmented plane-wave (FLAPW) method. In their calculation the VB width was ≈6 eV. The energy dispersion of the SBT unit cell by LDA<sup>5,6</sup> differs from that by TB.<sup>2</sup> However, Stachiotti et al.<sup>5,6</sup> showed no detailed structure around the conduction band minimum (CBM), demonstrating which of the Bi p and Ta d states has lower energy. Tsai and Dey<sup>7</sup> carried out the electronic structure computation based on the pseudofunction method. Their calculation for SBT indicated metallic DOS in which an energy gap was absent in the vicinity of the Fermi level.

As summarized above, detailed electronic structure of SBT is still controversial; nevertheless, the electronic

\* To whom correspondence should be addressed. E-mail: koiki@che.kyutech.ac.jp.

(1) Paz de Araujo, C. A.; Cuchiaro, J. D.; McMillan, L. D.; Scott, M. C.; Scott, J. F. *Nature* **1995**, *374*, 627.

(2) Robertson, J.; Chen, C. W.; Warren, W. L.; Gutleben, C. D. *Appl. Phys. Lett.* **1996**, *69*, 1704.

(3) Hartmann, A. J.; Lamb, R. N.; Scott, J. F.; Gutleben, C. D. *Integr. Ferroelectr.* **1997**, *18*, 101.

(4) Watanabe, K.; Hartmann, A. J.; Lamb, R. N.; Craig, R. P.; Thurgate, S. M.; Scott, J. F. *Jpn. J. Appl. Phys.* **2000**, *39*, L309.

(5) Stachiotti, M. G.; Rodriguez, C. O.; Ambrosch-Draxl, C.; Christensen, N. E. *Ferroelectrics* **2000**, *237*, 49.

(6) Stachiotti, M. G.; Rodriguez, C. O.; Ambrosch-Draxl, C.; Christensen, N. E. *Phys. Rev.* **2000**, *B61*, 14434.

(7) Tsai, M. H.; Dey, S. K. *IEEE Trans. Ultrason. Ferroelectr. Freq. Control* **2000**, *47*, 929.

nature depends only on the structure of the unit cell. The crystal structure of SBT, consisting of both double Sr-Ta-O perovskite blocks and  $\text{Bi}_2\text{O}_3$  layers, is orthorhombic ( $a = 0.5531$ ,  $b = 0.5534$ , and  $c = 2.4984$  nm).<sup>8</sup> The primitive cell includes 28 atoms. The structure containing one formula unit in a primitive cell can be described in terms of relatively small perturbations from a high-symmetry body-centered tetragonal structure ( $I4/mmm$ ,  $a = b = 0.391$  nm) as pointed out by Stachiotti et al.<sup>5,6</sup>

In this work we present both experimental and theoretical studies of the electronic structure of SBT. The Curie temperature ( $T_c$ ) of our SBT powder sample was 310 °C. The crystal structure and chemical state in both bulk and surface were examined by X-ray diffraction (XD), Raman spectroscopy (RS), and XPS. From bulk to surface the powder sample was SBT, having no excess Bi and/or  $\text{Bi}_2\text{O}_3$ . The theoretical VB spectrum, deduced from the DOS by FLAPW calculation and the photoionization cross section, reproduced well the experimental VB spectrum. The valence band maximum (VBM) is dominated by the O p states. The low-energy part of the CB is formed from the Bi p and Ta d states hybridizing with the O p states. We showed first that the Bi p states have slightly lower energy than the Ta d states and the hybridization between Bi p states and Ta d states is weak in the vicinity of the CBM.

## II. Experiment and Computation

We have synthesized an SBT powder sample from the 0.005 mol/L precursor solution, prepared by dissolving strontium oxalate monohydrate, bismuth chloride, and tantalum chloride into absolute ethanol, drying, and calcining in flowing oxygen at 800 °C for 3 h. For the sample we have measured XD and RS using a Rigaku CN2013 diffractometer and a JASCO NR-1800 spectrometer, respectively. XPS was performed by using a Surface Science Laboratories Model SSX-100 spectrometer with a monochromatized Al K $\alpha$  source. The spectrometer was calibrated utilizing the Au 4f<sub>7/2</sub> electrons (83.79 eV) and the full width at half-maximum (fwhm) of the Au 4f<sub>7/2</sub> peak was 1.03 eV. Charging effects were corrected with the C 1s photoelectron peak (285.0 eV). The experimental uncertainty amounted to  $\pm 0.15$  eV.

We have performed first-principles electronic structure calculations for both an ideal tetragonal unit cell without ferroelectric distortion and an experimentally determined orthorhombic one. The former has been used by Stachiotti et al.<sup>6</sup> Following their calculations, the atomic positions are taken from ref 6 as listed in Table 1. The atomic positions for orthorhombic structure are taken from the experimental data by Shimakawa et al.,<sup>8</sup> which are listed in Table 2.

The electronic structure calculations have been performed by the FLAPW method (WIEN97 code)<sup>9</sup> within the local density approximation. The muffin-tin sphere radii  $R_i = 2.0$ , 2.3, 1.8, and 1.5 au were used for Sr, Bi, Ta, and O, respectively. The  $R_{\text{K}_{\text{max}}}$  value, controlling the size of the basis set for the wave functions, of 7.0 used in all the calculations resulted in well-converged basis sets consisting of approximately 2200 LAPW functions for a tetragonal structure and 4500 for an orthorhombic one.

(8) Rae, A. D.; Thompson, J. G.; Withers, R. L. *Acta Crystallogr. B* **1992**, *48*, 418. Shimakawa, Y.; Kubo, Y.; Nakagawa, Y.; Goto, S.; Kamiyama, T.; Asano, H.; Izumi, F. *Phys. Rev. B* **2000**, *61*, 6559.

(9) Blaha, P.; Schwarz, K.; Luitz, J. *WIEN97, A Full Potential Linearized Augmented Plane Wave Package for Calculating Crystal Properties*; Karlheinz Schwarz, Techn. Universität Wien, Austria, 1999.

**Table 1. Atomic Coordinates<sup>a</sup>**

atom	<i>X</i>	<i>Y</i>	<i>Z</i>	atom	<i>X</i>	<i>Y</i>	<i>Z</i>
Sr	0	0	0	O(1)	0.5	0.5	0
Bi	0	0	0.20124	O(2)	0.5	0.5	0.16033
Ta	0.5	0.5	0.08468	O(3)	0	0.5	0.25
				O(4)	0	0.5	0.07602

<sup>a</sup> O(1), O(2), and O(3) represent oxygen atoms at the site in the Sr-O sheet sandwiched between the double Ta-O(4) sheets, at the site between the Bi sheet and Ta-O(4) sheet, and at the site of the O sheet sandwiched between the double Bi sheets, respectively. O(4) contains both the (100) and the (010) sites in the  $\text{TaO}_4$  sheet of  $\text{TaO}_6$  octahedra. Displacement of ions along the [110] direction in the tetragonal structure should be responsible for the macroscopic spontaneous polarization along the *a* direction of the orthorhombic cell observed below  $T_c$ .

**Table 2. Atomic Coordinates<sup>a</sup>**

atom	<i>X</i>	<i>Y</i>	<i>Z</i>	atom	<i>X</i>	<i>Y</i>	<i>Z</i>
Sr	0	0.2567	0	O(1)	0.5248	0.2892	0.0
Bi	0.4634	0.7764	0.19996	O(2)	0.5219	0.6990	0.34187
Ta	0.5104	0.7480	0.41482	O(3)	0.7381	0.9923	0.25076
				O(4)	0.7554	0.9867	0.06964
				O(5)	0.7909	0.9807	0.58359

<sup>a</sup> Atomic coordinates for orthorhombic SBT. The orthorhombic distortion splits the O(4) sites of the tetragonal structure into two inequivalent sites, O(4) and O(5).

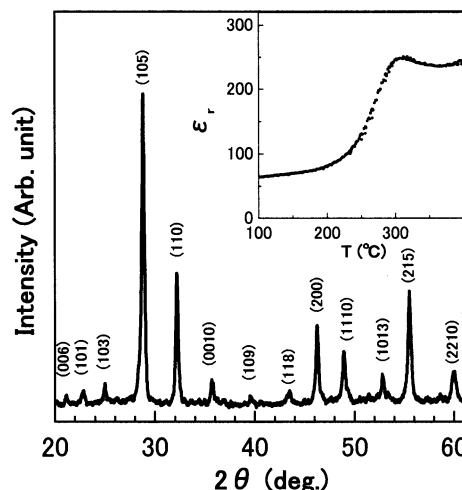


**Figure 1.** X-ray diffraction pattern with Cu K $\alpha$  radiation. Inset: Temperature dependence of the dielectric constant at 5 kHz.

## III. Results and Discussion

Temperature dependence of the dielectric constant of the powder sample is shown in the inset of Figure 1. A maximum observed at 310 °C matches well with the reported  $T_c$  of SBT.<sup>10</sup> The XD pattern in Figure 1 and RS spectrum in Figure 2 agreed well with those of SBT reported in refs 11 and 12, respectively. These agreements suggest that the powder sample preserved the translational symmetry of the SBT crystal structure from bulk to surface. As illustrated in Figure 3, core-level XPS spectra revealed that even at the surface of powders there is no metallic Bi. As mentioned above, the synthesized powders conserved the symmetry of the

(10) *Landolt-Bornstein*, New Series; Hellwege, K. H., Ed.; Springer-Verlag: Berlin, 1981; Vol. 16, pp 235.

(11) Lee, J. S.; Kim, H. H.; Kwon, H. J.; Jeong, Y. W. *Appl. Phys. Lett.* **1998**, *73*, 166.

(12) Graves, P. R.; Hua, G.; Myhra, S.; Thompson, J. G. *J. Solid State Chem.* **1995**, *114*, 112.

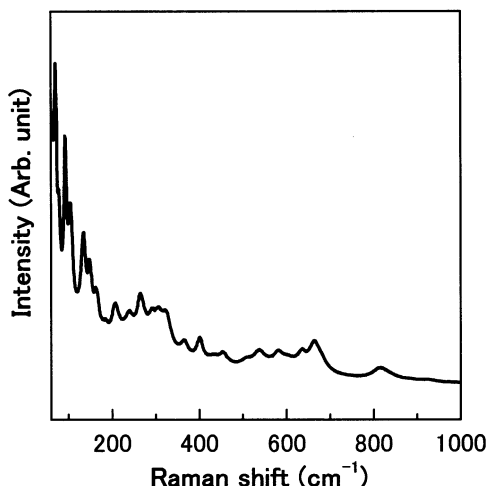


**Figure 2.** Raman spectrum measured in the backscattering geometry with  $\text{Ar}^+$  (514.5 nm and 300 mW) excitation.

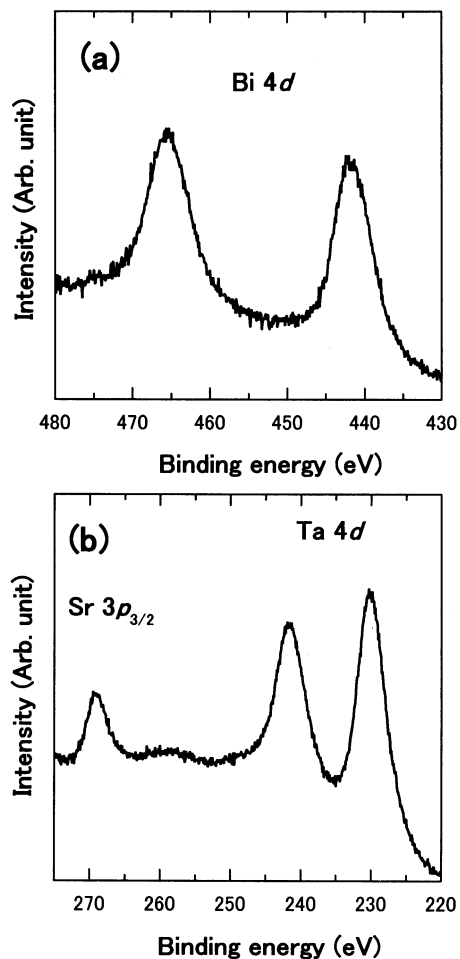


**Figure 3.** Core-level X-ray photoemission spectra of Bi (a) and of Ta with Sr (b) measured in a vacuum of  $4 \times 10^{-10}$  Torr at room temperature.

SBT crystal structure from bulk to surface, and the SBT powder surfaces have never been covered with metallic Bi and  $\text{Bi}_2\text{O}_3$ . As pointed out by Palanduz and Smyth,<sup>13</sup> metallic Bi must be formed in the alkoxide-based solution deposition process on the surface of the SBT film. Therefore, the VB spectrum by XPS of this powder

sample deserves to be compared with the theoretical VB spectrum derived from the DOS computed by the FLAPW method<sup>9</sup> and the photoionization cross section.<sup>14</sup>

As a first step for deriving the theoretical VB spectrum, the DOSs of SBT were calculated (Figure 4). For the tetragonal structure, they agree with the previous calculations.<sup>6</sup> The total and site-decomposed DOS suggest that the O 2p character hybridizing strongly with Bi and Ta states is predominant in the VB above  $-6$  eV and is substantial also in the CB above 2 eV, which is dominated by the states from Bi and Ta. The DOS at around  $-10$  eV is due to the Bi 6s states.

Orthorhombic distortion affects the electronic structures. The distortion changes the bond angle of O(4)–Ta–O(4) from the ideal  $180^\circ$ . It may cause the decrease of effective hybridization between O 2p and Ta 5d orbitals, resulting in narrower valence bands for the orthorhombic structure. From Figure 5, it is found that the valence bandwidth of the orthorhombic structure is about 0.2 eV narrower than that of the tetragonal structure, which is consistent with the expectation. The orthorhombic distortion also increases the energy gap from 2 eV for the tetragonal structure to 2.5 eV for the orthorhombic one.

The theoretical VB spectrum without broadening depicted by Figure 5a was derived from the DOS and the photoionization cross section.<sup>14</sup> The spectra of parts b and c of Figure 5 are broadened with the Gaussian functions of fwhm's of 0.4 and 1.0 eV, respectively, for convenience of comparison with the experiment. As seen, the Gaussian broadening by larger fwhm brings about a wider VB, where the detailed structure in the DOS was smoothed out. By the 1.0 eV–fwhm broadening the VB was widened to approximately 8 eV. The energy splitting between the VB and the semicore state remained at  $\approx 7$  eV.

As depicted by Figure 5d, the experimental VB spectrum can be approximated by two Gaussian components: a major part centered at 4 eV and a minor part at around 11 eV. The major part represents the VB consisting of the states from Sr, Bi, Ta, and O, whereas the minor part is due to the Bi 6s semicore state. The energy difference between the two components was  $\approx 7$  eV. The VB width, determined from both intercepts of linear fits to the left and right shoulders of the peak with the zero line, was 8.5 eV. The experimental bandwidth (8.5 eV) agreed well with that of theory (8 eV). It is well-known that the VB width calculated is somewhat narrower with respect to that from experiment because the experimental spectrum is affected largely by the energy broadening due to the electron spectrometer and the X-ray line width for excitation. The energy splittings between the VB and the Bi 6s state of the experiment and theory agreed well with each other.

The VBM is dominated by O 2p states hybridizing with Ta 5d states, which is a common feature of transition metal oxides with an octahedral oxygen cage. On the other hand, the CBM has contribution from both Ta d and Bi p states. To clarify the nature of conduction bands, we plotted the energy bands with the character

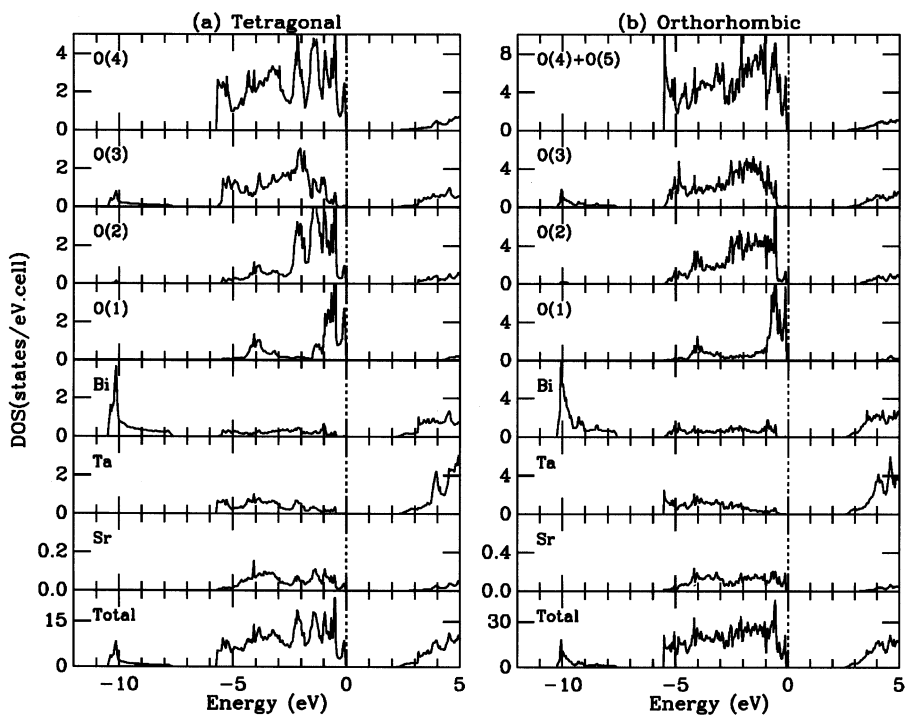


**Figure 4.** Total and site-decomposed all electron density of states of  $\text{SrBi}_2\text{Ta}_2\text{O}_9$  for tetragonal (a) and orthorhombic (b) structure. The contribution from Sr states is very small. Note the magnitude of order.

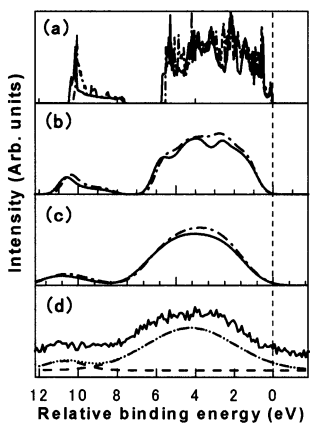


**Figure 5.** Theoretical valence band spectra derived from the DOS (Figure 4) and the photoionization cross section without broadening (a) and broadened with the Gaussian functions fwhm's of 0.4 (b) and 1.0 eV (c). The spectra for tetragonal and orthorhombic structures are shown by solid and dash-dotted lines, respectively. The broadened spectra are shifted by (b) 0.5 eV and (c) 1.0 eV so that the tails of spectra are adjusted at the origin of relative binding energy. The experimental valence band spectrum is shown in (d), where the quadratic background was subtracted. The dotted line, parallel to the experimental spectrum, represents the sum of two Gaussian components depicted by broken lines.

of wave functions for the tetragonal structure. As demonstrated in Figure 6, we found that the energy bands near the CBM can be classified into two kinds of states. The one is formed mainly from Bi 6p and O 2p states and the second is from Ta 5d and O 2p states. Since these two kinds of states exist at spatially different atomic sites, mixing between them are small, near CBM. The Bi 6p derived states have lower energy between these two kinds of states. Thus, the energy gap is between VBM composed of Ta 5d and O 2p states and CBM of Bi 6p and O 2p states. We have verified that

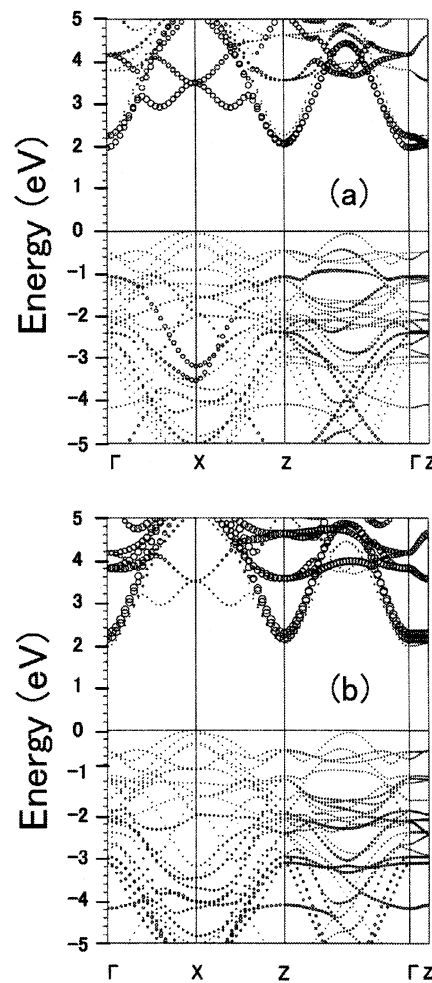


**Figure 6.** Energy bands of tetragonal SBT in the vicinity of the conduction band minimum. The circles indicate the weights of wave functions projected to the sites of Bi (a) and Ta (b).

these characterizations are unchanged for the orthorhombic structure with ferroelectric distortions.

#### IV. Summary

We have synthesized SBT powders with a  $T_c$  of 310 °C from the 0.005 mol/L precursor solution. XD, RS, and XPS showed that the crystal structure of SBT was preserved from bulk to surface of the powder sample, and the surface has never been covered with metallic Bi and/or  $Bi_2O_3$ . Theoretical VB spectrum derived from the DOS by FLAPW computation with the photoionization cross section reproduced well the experimental spectrum. The DOS revealed that the VBM dominated by the O p states departs from the CBM where the Bi

p and Ta d states are hybridizing with the O p states. The Bi p state has lower energy than the Ta d state. The orthorhombic structure shows a larger energy gap and slightly narrower valence bands than the tetragonal one without ferroelectric distortion.

**Acknowledgment.** S.T. is grateful for the support by the Sasakawa Scientific Research Grant from the Japan Science Society. S.K. is thankful for the support of The Corning Japan Research Grant for this work. A part of this work was performed under the interuniversity cooperative research program of the Laboratory for Advanced Materials, the Institute for Materials Research, Tohoku University.

CM020353S